

Exploring Scalar and Vector Bileptons at the LHC in a 331 Model

Gennaro Corcella^a, Claudio Corianò^b, Antonio Costantini^b, Paul H. Frampton^b

^a*INFN, Laboratori Nazionali di Frascati,
Via E. Fermi 40, 00044, Frascati (RM), Italy*

^b*Dipartimento di Matematica e Fisica ‘Ennio De Giorgi’, Università del Salento and INFN, Sezione di Lecce,
Via Arnesano, 73100 Lecce, Italy*

Abstract

We present an analysis on the production of two same-sign lepton pairs at the LHC, mediated by bileptons in the $SU(3)_c \times SU(3)_L \times U(1)_X$ theory, the so-called 331 model. Compared to other 331 scenarios, in this model the embedding of the hypercharge is obtained with the addition of 3 exotic quarks and doubly-charged vector gauge bosons with lepton numbers ± 2 in the spectrum ($Y^{\pm\pm}$), which can mediate the production of four-lepton final states. Furthermore, a complete description of the model requires the introduction of a Higgs scalar sector, which is a sextet of $SU(3)_L$, necessary in order to correctly account for the lepton masses. As a result of this, new doubly-charged scalar states $H^{\pm\pm}$ are part of the spectrum as well and can in principle compete with the vector bileptons in giving rise to four-lepton final states. We investigate both channels and study several observables at the LHC, for both signal and Standard Model ZZ background. With respect to previous work on vector- and scalar-bilepton production, we use the most updated exclusion limits at the LHC and implement the 331 model in a full Monte Carlo simulation code, capable of being interfaced with any analysis framework. Our result is that the 331 signal can be discriminated from the background with a significance of 6-9 standard deviations, depending on the LHC luminosity, with the vector bileptons dominating over the scalar ones.

1. Introduction

In the experimental searches for new physics of the fundamental interactions at the LHC, the resolution of several open issues - which remain unanswered within the Standard Model (SM) - typically call for larger gauge structures and a wider particle content. Such are the gauge-hierarchy problem in the Higgs sector or the origin of light-neutrino masses, just to mention two of them, both requiring such extensions. Grand Unified Theories (GUTs) play certainly an important role in this: unfortunately, Grand Unification needs an energy scale $\mathcal{O}(10^{12}\text{-}10^{15})$ GeV, which is far higher than the electroweak one, currently probed at the LHC. Obviously, the process of identifying the main signatures of a certain symmetry-breaking pattern from the GUT scale down to the TeV scale is far from being trivial, due to the enlarged symmetries and to a parameter space of considerable

Email addresses: gennaro.corcella@lnf.infn.it (Gennaro Corcella), claudio.coriano@le.infn.it (Claudio Corianò), antonio.costantini@le.infn.it (Antonio Costantini), paul.h.frampton@gmail.com (Paul H. Frampton)

size. There are, however, interesting scenarios where larger gauge symmetries can be discovered or ruled out already at the TeV scale, which suggests some alternative paths of exploration. Such is the case of a version of the $SU(3)_c \times SU(3)_L \times U(1)_X$ model, also known as 331 model [1, 2, 3], where the requirement that the gauge couplings are real provides a significant upper bound on the physical region in which its signal could be searched for. This property sets the vacuum expectation values (vevs) of the Higgs bosons, which trigger the breaking from the 331-symmetry scale down to the electroweak one, around the TeV. The model that we consider allows for bileptons, i.e. gauge bosons (Y^{--}, Y^{++}) of charge $Q = \pm 2$ and lepton number $L = \pm 2$, and therefore we shall refer to it as the *bilepton model*. In the family of 331 models, bileptons in the spectrum are obtained only for special embeddings of the $U(1)_X$ symmetry and of the charge (Q) and hypercharge (Y) generators in the local gauge structure. One additional feature of the model is that, unlike the Standard Model or most chiral models formulated so far, extending the SM spectrum and symmetries, the number of (chiral) fermion generations is underwritten by the cancellation of the gauge anomalies. Gauge anomalies cancel among different fermion families, and select the number of generations to be 3: from this perspective, the model appears to be quite unique. Moreover, in the formulation of [1], which we shall adopt hereafter, the third fermion family is treated asymmetrically with respect to the first two families.

In a previous analysis [4] we have presented results for the production of pairs of vector bileptons ($Y^{++}Y^{--}$) decaying into two same-sign lepton pairs, in conjunction with two jets at the LHC, at $\sqrt{s} = 13$ TeV and relying on a full Monte Carlo implementation of the 331 model. Our study has been based on the selection of a specific benchmark point in the parameter space, where the Y bileptons have mass $m_Y \simeq 875$ GeV. We have shown that, by setting appropriate cuts on the rapidities and transverse momenta of the final-state leptons and jets, it is possible to suppress the Standard Model background. By including jets in the final state, one obtains larger signal/background ratio, but nonetheless one has to face the issue of jet reconstruction.

In this paper, we wish to extend the investigation in [4]. In fact, in [4] the explicit mass matrices of the scalars in a minimal version of the model, containing only 3 $SU(3)_L$ triplets, as well as the minimization conditions of the potential, were presented. However, the model also allows for doubly-charged Higgs-like scalars (H^{++}, H^{--}), which may give rise to multi-lepton final state, in the same manner as the vectors $Y^{\pm\pm}$ debated in [4]. We shall therefore explore the production of same-sign lepton pairs at the LHC, mediated by both scalar and vector bileptons; unlike Ref. [4], we shall veto final-state jets.

The production of doubly-charged vector bilepton pairs at the LHC in jetless Drell–Yan processes was already investigated in [5, 6, 7, 8]. In particular, the authors of [8] implemented the bilepton model in a full Monte Carlo simulation framework and obtained the exclusion limit $m_Y^{\pm\pm} > 850$ GeV, by using the ATLAS rates at $\sqrt{s} = 7$ TeV [9] on expected and observed high-mass same-sign lepton pairs and extending the results to 13 TeV and $\mathcal{L} = 50 \text{ fb}^{-1}$. However, the analysis in [8] assumes that the same-sign lepton-pair yields are independent of the bilepton spin: in fact, the ATLAS analysis in [9] was performed for scalar doubly-charged Higgs bosons, while the predictions in [8] concerned vector bileptons. It is precisely the goal of the present exploration understanding whether, referring to the 331 realization in [1], one can separate vector from scalar bileptons at the LHC, in different luminosity regimes. A careful investigation on the production of doubly-charged particles at the LHC and the dependence of final-state distributions on the spin was undertaken in [10]. The authors of [10] considered an effective simplified model where the SM is extended by means of a $SU(2)_L$ group and the scalar, fermion and vector doubly-charged particles lie in the

trivial, fundamental and adjoint representations of $SU(2)_L$, respectively. By looking at transverse-momentum and angular distributions and varying the bilepton mass between 150 and 350 GeV, it was found that it could be possible to distinguish at the LHC the particle spin.

Compared to our previous study, in the present paper we shall explore a complete version of the model which includes both the $SU(3)_L$ triplet Higgses and the newly added scalar sextet sector, which is necessary in order to account for the masses of the leptons. The inclusion of the scalar sextet opens up the decay channels $H^{\pm\pm} \rightarrow l^\pm l^\pm$, which compete with the companion $Y^{\pm\pm} \rightarrow l^\pm l^\pm$ process. Many of the analytic expressions in the description of the sextet contributions, such as the rotation matrices appearing in the extraction of the mass eigenstates of this sector, cannot be given in closed analytical form, since they would be too lengthy. As in [4] we shall choose a benchmark point of the model and present our results numerically: in particular, as we are interested in comparing vector- and scalar-bilepton signals, we shall set the doubly-charged Y^{++} and H^{++} masses to the same value.

Vector- and scalar-bilepton production at hadron colliders was also explored in [11], where the authors presented the total cross sections, expected number of events at the LHC, invariant-mass and transverse-momentum spectra for a few values of the bilepton mass. The decay properties of doubly-charged Higgs bosons in a minimal 331 model were also studied in [12]. It was found that, since the coupling to leptons is proportional to the lepton mass, such scalar bileptons mostly decay into τ -lepton pairs. Also, according to [12], the rate into WW pairs is suppressed, being proportional to the vacuum expectation value of the Higgs giving mass to the neutrinos, as well as decays into leptons of different flavours, since the Yukawa couplings are diagonal. While the investigation in [11] was performed at leading order, by using the **FORM** package [13] to calculate the amplitudes, we shall undertake a full hadron-level investigation. We will implement the 331 model, including the sextet sector, into **SARAH 4.9.3** [14], while the amplitudes for bilepton production at the LHC will be computed by the **MadGraph** code [15]; the simulation of parton showers and hadronization will be performed by using **HERWIG 6** [16]. Also, as will be thoroughly debated later on, in our model doubly-charged scalar bileptons decay in all lepton-flavour pairs with branching ratios $1/3$, unlike Ref. [12], wherein the $\tau^+\tau^-$ mode had the largest rate.

From the experimental viewpoint, to our knowledge, there has been no actual search for vector bileptons at the LHC, whereas the latest investigations on possible doubly-charged scalar Higgs boson production at the LHC were undertaken in [17] and [18] by ATLAS and CMS, respectively. In detail, the ATLAS analysis, performed at 13 TeV and with 36 fb^{-1} of data, considered the so-called left-right symmetric model (LRSM, see, e.g. Refs. [19, 20]) and its numerical implementation in [21], where doubly-charged Higgs bosons can couple to either left-handed or right-handed leptons. In this framework, assuming that the $H^{\pm\pm}$ bosons only decay into lepton pairs, exclusion limits were set in the range 770-870 GeV for $H_L^{\pm\pm}$ and 660-760 GeV for $H_R^{\pm\pm}$. As for CMS, a luminosity of 12.9 fb^{-1} was taken into account and limits between 800 and 820 were determined, always under the assumption of a 100% branching ratio into same-sign lepton pairs.

Our paper is organized as follows. In Section 2, we shall discuss the family embedding in the minimal 331 model, while Section 3 will be more specific on its scalar content, giving details on the triplet and sextet sectors, as well as on the lepton masses and physical Higgs bosons. Our phenomenological analysis will be presented in Section 5 and final comments and remarks will be given in Section 6.

2. Family embedding in the minimal 331

One of the main reasons for the appearance of exotic particles in the spectrum of the 331 model is the specific embedding of the hypercharge Y in the $SU(3)_L \times U(1)_X$ gauge symmetry. The embeddings of Y and of the charge operator Q_{em} are obtained by defining them as linear combinations of the diagonal generators of $SU(3)_L$. We recall that in the 331 case this is defined by

$$Y_{\mathbf{3}} = \beta T_8 + X \mathbf{1} \quad Y_{\bar{\mathbf{3}}} = -\beta T_8 + X \mathbf{1} \quad (1)$$

for the $\mathbf{3}$ and the $\bar{\mathbf{3}}$ representations of $SU(3)_L$, respectively, with generators $T_i = \lambda_i/2$ ($i = 1, \dots, 8$), corresponding to the Gell-Mann matrices, and $T_8 = \text{diag} \left[\frac{1}{2\sqrt{3}}(1, 1, -2) \right]$. The charge operator is given by

$$Q_{em, \mathbf{3}} = Y_{\mathbf{3}} + T_3 \quad Q_{em, \bar{\mathbf{3}}} = Y_{\bar{\mathbf{3}}} - T_3 \quad (2)$$

in the fundamental and anti-fundamental representations of $SU(3)_L$, respectively, where we have $T_3 = \text{diag} \left[\frac{1}{2}(1, -1, 0) \right]$. We choose the $SU(2)_L \times U(1)_Y$ hypercharge assignments of the Standard Model as $Y(Q_L) = 1/6$, $Y(L) = -1/2$, $Y(u_R) = 2/3$, $Y(d_R) = -1/3$ and $Y(e_R) = -1$. Denoting by q_X the particle charges under $U(1)_X$, the breaking of the symmetry $SU(3)_L \times U(1)_X \rightarrow SU(2)_L \times U(1)_Y$, for the fundamental representation $\mathbf{3}$ reads

$$(\mathbf{3}, q_X) \rightarrow \left(2, \frac{\beta}{2\sqrt{3}} + q_X \right) + \left(1, -\frac{\beta}{\sqrt{3}} + q_X \right), \quad (3)$$

while for the representation $\bar{\mathbf{3}}$

$$(\bar{\mathbf{3}}, q'_X) \rightarrow \left(2, -\frac{\beta}{2\sqrt{3}} + q'_X \right) + \left(1, +\frac{\beta}{\sqrt{3}} + q'_X \right). \quad (4)$$

The X -charge is fixed by the condition that the first two components of the Q_1 and Q_2 triplets carry the same hypercharge as the quark doublets $Q_L = (u, d)_L$ of the Standard Model, yielding

$$q_X = \frac{1}{6} - \frac{\beta}{2\sqrt{3}}. \quad (5)$$

The $U(1)_{em}$ charge of the triplet will then be $Q_{em}(Q_1) = \text{diag}(2/3, -1/3, 1/6 - \sqrt{3}\beta/2)$. Fermions with exotic charges will be automatically present in the case of $\beta = \sqrt{3}$, which is the parameter choice that we will consider hereafter in our analysis. The first two families will then be assigned as

$$Q_1 = \begin{pmatrix} u_L \\ d_L \\ D_L \end{pmatrix}, \quad Q_2 = \begin{pmatrix} c_L \\ s_L \\ S_L \end{pmatrix}, \quad Q_{1,2} \in (\mathbf{3}, \mathbf{3}, -1/3) \quad (6)$$

under $SU(3)_c \times SU(3)_L \times U(1)_X$. The charge operator Q_{em} on $Q_{1,2}$ will then give

$$Q_{em}(Q_{1,2}) = \text{diag}(2/3, -1/3, -4/3), \quad (7)$$

with two exotic quarks D and S of charge $-4/3$. The third family is instead assigned as

$$Q_3 = \begin{pmatrix} b_L \\ t_L \\ T_L \end{pmatrix}, \quad Q_3 \in (\mathbf{3}, \bar{\mathbf{3}}, 2/3), \quad (8)$$

where the hypercharge content of the third exotic quark (T_L) is derived from the operator ($Y_{\bar{\mathbf{3}}}$)

$$Y_{\bar{\mathbf{3}}}(Q_3) = \text{diag} \left(-\frac{\beta}{2\sqrt{3}} + q'_X, -\frac{\beta}{2\sqrt{3}} + q'_X, \frac{\beta}{\sqrt{3}} + q'_X \right), \quad (9)$$

with the condition $q'_X = 1/6 + \beta/(2\sqrt{3})$, giving

$$Y_{\bar{\mathbf{3}}}(Q_3) = \text{diag} \left(\frac{1}{6}, \frac{1}{6}, \frac{5}{3} \right) \quad (10)$$

and

$$Q_{em\bar{\mathbf{3}}}(Q_3) = \text{diag} \left(-\frac{1}{3}, \frac{2}{3}, \frac{5}{3} \right). \quad (11)$$

With these assignments, the charge of T_L is $Q_{em}(T_L) = 5/3$, allowing to distinguish between the third and the first two generations of quarks. Right-handed singlet quarks in the 331 model carry the usual SM charges ($2/3$ and $-1/3$ for the u -type and d -type quarks),

$$(d_R, s_R, b_R) \in (\mathbf{3}, 1, -1/3) \quad (12)$$

$$(u_R, c_R, t_R) \in (\mathbf{3}, 1, 2/3), \quad (13)$$

$$(14)$$

with the exception of the three right-handed exotics

$$(D_R, S_R) \in (\mathbf{3}, 1, -4/3) \quad (15)$$

$$T_R \in (\mathbf{3}, 1, 5/3). \quad (16)$$

The lepton sector is assigned to the representation $\bar{\mathbf{3}}$ of the same gauge group. Conversely from the quark sector, there is a democratic arrangement of the three lepton generations into triplets of $SU(3)_L$,

$$l = \begin{pmatrix} e_L \\ \nu_L \\ e_R^c \end{pmatrix}, \quad l \in (\mathbf{1}, \bar{\mathbf{3}}, 0), \quad (17)$$

with $e_R^c = i\sigma_2 e_R^*$. In the following, we shall adopt for the leptons the notation l_a^i , where the subscripts (a, b or c) refer to the lepton generation (electrons, muons and taus), and the superscripts ($i, j, k = 1, 2, 3$) are $SU(3)_L$ indices. For example, the generation a corresponds to electrons and the three elements of the triplet (17) are labelled as:

$$l_a^1 = e_{aL}, \quad l_a^2 = \nu_{aL}, \quad l_a^3 = e_{aR}^c. \quad (18)$$

For the hypercharge operator we have the decomposition under $SU(2)_L \times U(1)_Y$

$$Y_{\bar{\mathbf{3}}}(l) = \left(-\frac{\beta}{2\sqrt{3}} + q''_X, -\frac{\beta}{2\sqrt{3}} + q''_X, \frac{\beta}{\sqrt{3}} + q''_X \right) \quad (19)$$

with $q''_X = 1/6 + \beta/(2\sqrt{3})$ and $Q_{em}(L) = \text{diag}(-1, 0, 1)$. Both left- and right-handed components of the SM leptons are fitted into the same $SU(3)_L$ multiplet.

The scalars of the 331 model, responsible for the electroweak symmetry breaking (EWSB), come in three triplets of $SU(3)_L$:

$$\rho = \begin{pmatrix} \rho^{++} \\ \rho^+ \\ \rho^0 \end{pmatrix} \in (1, 3, 1), \quad \eta = \begin{pmatrix} \eta^+ \\ \eta^0 \\ \eta^- \end{pmatrix} \in (1, 3, 0), \quad \chi = \begin{pmatrix} \chi^0 \\ \chi^- \\ \chi^{--} \end{pmatrix} \in (1, 3, -1). \quad (20)$$

The breaking $SU(3)_L \times U(1)_X \rightarrow U(1)_{em}$ is obtained in two steps. The vacuum expectation value of the neutral component of ρ causes the breaking from $SU(3)_L \times U(1)_X$ to $SU(2)_L \times U(1)_Y$; the usual spontaneous symmetry breaking mechanism from $SU(2)_L \times U(1)_Y$ to $U(1)_{em}$ is then obtained through the vevs of the neutral components of η and χ .

Before closing this section, we remind that in the models [1, 2] the coupling constants of $SU(3)_L$ and $U(1)_X$, namely g_{3L} and g_X , are related to the electroweak mixing angle θ_W in such a way that $g_X(\mu)$ exhibits a Landau pole at a scale μ whenever $\sin^2 \theta_W(\mu) = 1/4$ [24].¹ Therefore, the theory may lose its perturbativity even at the scale about 3.5 TeV [25]. Nevertheless, the typical energy scale of bilepton-pair production in [4] and in this paper is somewhat smaller, i.e. $2m_{Y\pm\pm} \simeq 1.75$ TeV. Therefore, we shall assume that the Landau pole does not pose any threat to the perturbative analysis carried out in the present work.

3. The scalar sectors

The model presented in the previous section exhibits the interesting feature of having both scalar and vector doubly-charged bosons, which is a peculiarity of the minimal version of the 331 model. In fact it is possible to consider various versions of the $SU(3)_c \times SU(3)_L \times U(1)_X$ gauge symmetry, usually parametrized by β [22]. We discuss the case of $\beta = \sqrt{3}$, corresponding to the minimal version presented here, leading to vector boson with electric charge equal to ± 2 . Doubly-charged states are interesting by themselves because they can have distinctive features in terms of allowed decay channels, for example the production of same-sign lepton pairs. In the context of the minimal 331 model there is an even more interesting possibility. In fact, one can test whether a same-sign lepton pair has been produced by either a scalar or a vector boson. As we are going to explain, this feature will also shed light on the presence of a higher representation of the $SU(3)_c \times SU(3)_L \times U(1)_X$ gauge group, namely the sextet.

3.1. The triplet sector

In the previous section we have seen that the EWSB mechanism is realised in the 331 model by giving a vev to the neutral component of the triplets ρ , η and χ . The Yukawa interactions for SM and exotic quarks are obtained by means of these scalar fields and are given by:

$$\begin{aligned} \mathcal{L}_{q,triplet}^{Yuk.} = & (y_d^1 Q_1 \eta^* d_R + y_d^2 Q_2 \eta^* s_R + y_d^3 Q_3 \chi b_R^* \\ & + y_u^1 Q_1 \chi^* u_R^* + y_u^2 Q_2 \chi^* c_R^* + y_u^3 Q_3 \eta t_R^* \\ & + y_E^1 Q_1 \rho^* D_R^* + y_E^2 Q_2 \rho^* S_R^* + y_E^3 Q_3 \rho T_R^*) + \text{h.c.}, \end{aligned} \quad (21)$$

¹The relation between the $SU(3)_L$ and $U(1)_X$ couplings reads: $g_X^2/g_{3L}^2 = \sin^2 \theta_W / (1 - 4 \sin^2 \theta_W)$ [24, 25].

where y_d^i , y_u^i and y_E^i are the Yukawa couplings for down-, up-type and exotic quarks, respectively. The masses of the exotic quarks are related to the vev of the neutral component of $\rho = (0, 0, v_\rho)$ via the invariants

$$\begin{aligned} Q_1 \rho^* D_R^*, Q_1 \rho^* S_R^* &\sim (3, 3, -1/3) \times (1, \bar{3}, -1) \times (\bar{3}, 1, 4/3) \\ Q_3 \rho T_R^* &\sim (3, \bar{3}, 2/3) \times (1, 3, 1) \times (\bar{3}, 1, -5/3), \end{aligned} \quad (22)$$

responsible of the breaking $SU(3)_c \times SU(3)_L \times U(1)_X \rightarrow SU(3)_c \times SU(2)_L \times U(1)_Y$. It is clear that, being $v_\rho \gg v_{\eta, \chi}$, the masses of the exotic quarks are $\mathcal{O}(\text{TeV})$ whenever the relation $y_E^i \sim 1$ is satisfied.

3.2. The sextet sector

The need for introducing a sextet sector can be summarised as follows. A typical Dirac mass term for the leptons in the SM is associated with the operator $\bar{l}_L H e_R$, with $l_L = (v_{eL}, e_L)$ being the $SU(2)_L$ doublet, with the representation content $(\bar{2}, 1/2) \times (2, 1/2) \times (1, -1)$ (for l, H and e_R , respectively) in $SU(2)_L \times U(1)_Y$. In the 331 the L and R components of the lepton (e) are in the same multiplet and therefore the identification of an $SO(1, 3) \times SU(3)_L$ singlet needs two leptons in the same representation. It can be obtained (at least in part) with the operator

$$\begin{aligned} \mathcal{L}_{l, \text{triplet}}^{Yuk} &= G_{ab}^\eta (l_{a\alpha}^i \epsilon^{\alpha\beta} l_{b\beta}^j) \eta^{*k} \epsilon^{ijk} + \text{h.c.} \\ &= G_{ab}^\eta l_a^i \cdot l_b^j \eta^{*k} \epsilon^{ijk} + \text{h.c.} \end{aligned} \quad (23)$$

where the indices a and b run over the three generations of flavour, α and β are Weyl indices contracted in order to generate an $SO(1, 3)$ invariant ($l_a^i \cdot l_b^j \equiv l_{a\alpha}^i \epsilon^{\alpha\beta} l_{b\beta}^j$) from two Weyl fermions, and $i, j, k = 1, 2, 3$, are $SU(3)_L$ indices. The use of η as a Higgs field is mandatory, since the components of the multiplet l^j are $U(1)_X$ singlets. The representation content of the operator $l_a^i l_b^j$ according to $SU(3)_L$ is given by $3 \times 3 = 6 + \bar{3}$, with the $\bar{3}$ extracted by an anti-symmetrization over i and j via ϵ^{ijk} . This allows to identify $l_a^i l_b^j \eta^{*k} \epsilon^{ijk}$ as an $SU(3)_L$ singlet. Considering that the two leptons are anticommuting Weyl spinors, and that the $\epsilon^{\alpha\beta}$ (Lorentz) and ϵ^{ijk} ($SU(3)_L$) contractions introduce two sign flips under the $a \leftrightarrow b$ exchange, the combination

$$M_{ab} = (l_a^i \cdot l_b^j) \eta^{*k} \epsilon^{ijk} \quad (24)$$

is therefore antisymmetric under the exchange of the two flavours, implying that even G_{ab} has to be antisymmetric. However, an antisymmetric G_{ab}^η is not sufficient to provide mass to all leptons.

In fact, the diagonalization of G^η by means a unitary matrix U , namely $G^\eta = U \Lambda U^\dagger$, with G^η antisymmetric in flavour space, implies that its 3 eigenvalues are given by $\Lambda = (0, \lambda_{22}, \lambda_{33})$, with $\lambda_{22} = -\lambda_{33}$, i.e. one eigenvalue is null and the other two are equal in magnitude. At the minimum of η , i.e. $\eta = (0, v_\eta, 0)$, one has:

$$G_{ab}^\eta M^{ab} = -\text{Tr}(\Lambda U M U^\dagger) = 2v_\eta \lambda_{22} U_{2a} l_a^1 \cdot l_b^3 U_{2b}^* + 2v_\eta \lambda_{33} U_{3a} l_a^1 \cdot l_b^3 U_{3b}^*, \quad (25)$$

with $l_a^1 = e_{aL}$ and $l_b^3 = e_{bR}^c$. Introducing the linear combinations

$$E_{2L} \equiv U_{2a} l_a^1 = U_{2a}^c e_{aL}, \quad U_{2b}^* l_b^3 = U_{2b}^c e_{bR}^c = i\sigma_2 (U_{2b} e_{bR})^* \equiv E_{2R}^c, \quad (26)$$

then the antisymmetric contribution in flavour space becomes

$$\mathcal{L}_{l, \text{triplet}}^{Yuk} = 2v_\eta \lambda_{22} (E_{2L} E_{2R}^c - E_{3L} E_{3R}^c), \quad (27)$$

which is clearly insufficient to generate the lepton masses of three non-degenerate lepton families. We shall solve this problem by introducing a second invariant operator, with the inclusion of a sextet σ :

$$\sigma = \begin{pmatrix} \sigma_1^{++} & \sigma_1^+/\sqrt{2} & \sigma^0/\sqrt{2} \\ \sigma_1^+/\sqrt{2} & \sigma_1^0 & \sigma_2^-/\sqrt{2} \\ \sigma^0/\sqrt{2} & \sigma_2^-/\sqrt{2} & \sigma_2^{--} \end{pmatrix} \in (1, 6, 0), \quad (28)$$

leading to the Yukawa term

$$\mathcal{L}_{l, \text{sextet}}^{Yuk.} = G_{ab}^\sigma l_a^i \cdot l_b^j \sigma_{i,j}^*, \quad (29)$$

which allows to build a singlet out of the representation 6 of $SU(3)_L$, contained in $l_a^i \cdot l_b^j$, by combining it with the flavour-symmetric σ^* , i.e. $\bar{6}$. Notice that G_{ab}^σ is symmetric in flavour space.

It is interesting to note that if one did not consider the sextet it would not be possible for a doubly-charged scalar to decay into same-sign leptons. In fact, if we leave aside the sextet contribution, the Yukawa for the leptons is related to the scalar triplet η which does not possess any doubly-charged state. This means that revealing a possible decay $H^{\pm\pm} \rightarrow l^\pm l^\pm$ would be a distinctive signature of the presence of the sextet representation in the context of the 331 model.

3.3. Lepton Mass Matrices

The lepton mass matrices are of course related to the Yukawa interactions by the Lagrangian

$$\mathcal{L}_l^{Yuk.} = \mathcal{L}_{l, \text{sextet}}^{Yuk.} + \mathcal{L}_{l, \text{triplet}}^{Yuk.} + \text{h.c.} \quad (30)$$

and are combinations of triplet and sextet contributions. The structure of the mass matrix that emerges from the vevs of the neutral components of η and σ is thus given by:

$$\mathcal{L}_l^{Yuk.} = \left(\sqrt{2}\sigma_0 G_{a,b}^\sigma + 2v_\eta G_{ab}^\eta \right) (e_{aL} \cdot e_{bR}) + \sigma_1^0 G_{ab}^\sigma (\nu_L^T i\sigma_2 \nu_L) + \text{h.c.}, \quad (31)$$

which generates a Dirac mass matrix for the charged leptons M_{ab}^l and a Majorana mass matrix for neutrinos $M_{ab}^{\nu_l}$:

$$M_{ab}^l = \sqrt{2}\langle\sigma_0\rangle G_{a,b}^\sigma + 2v_\eta G_{ab}^\eta, \quad M_{ab}^{\nu_l} = \langle\sigma_1^0\rangle G_{ab}^\sigma. \quad (32)$$

In the expression above $\langle\sigma^0\rangle$ and $\langle\sigma_1^0\rangle$ are the vacuum expectation values of the neutral components of σ . For a vanishing G^σ , as we have already discussed, we will not be able to generate the lepton masses consistently, nor any mass for the neutrinos, i.e.

$$M_{ab}^l = 2v_\eta G_{ab}^\eta, \quad M^{\nu_l} = 0. \quad (33)$$

On the contrary, in the limit $G^\eta \rightarrow 0$, Eq. (32) becomes

$$M_{ab}^l = \sqrt{2}\langle\sigma_0\rangle G_{ab}^\sigma, \quad M_{a,b}^{\nu_l} = \frac{\langle\sigma_1^0\rangle}{\sqrt{2}} G_{ab}^\sigma, \quad (34)$$

which has some interesting consequences. Since the Yukawa couplings are the same for both leptons and neutrinos, we have to require $\langle\sigma_1^0\rangle \ll \langle\sigma^0\rangle$, in order to obtain small neutrino masses. For the goal of our analysis, we will assume that the vev of σ_1^0 vanishes, i.e. $\langle\sigma_1^0\rangle \equiv 0$. Clearly, if the matrix G^σ is diagonal in flavour space, from Eq. (34) we will immediately conclude that the Yukawa

coupling G^σ has to be chosen to be proportional to the masses of the SM leptons. An interesting consequence of this is that the decay $H^{\pm\pm} \rightarrow l^\pm l^\pm$, which is also proportional to G^σ , and therefore to the lepton masses, will be enhanced for the heavier leptons, in particular for the τ , as thoroughly discussed in [12]. This is an almost unique situation which is not encountered in other models with doubly-charged scalars decaying into same-sign leptons [21].

However, for the sake of generality, in the following analysis we will consider the most generic scenario where both contributions G^σ and G^η are present. In this case the branching ratios of the doubly-charged Higgs decaying into same-sign leptons do not have to be proportional to the masses of the lepton anymore. In particular, after accounting for both G^σ and G^η , configurations wherein even scalar bileptons have the same rates into the three lepton species are allowed, as occurs for vector bileptons. In the following, we shall hence concentrate our investigation on scenarios yielding

$$\text{BR}(Y^{\pm\pm} \rightarrow l^\pm l^\pm) \simeq \text{BR}(H^{\pm\pm} \rightarrow l^\pm l^\pm) \simeq 1/3 \quad (35)$$

for $l = e, \mu, \tau$. The condition in Eq. (35) is in fact particularly suitable to compare vector- and scalar-bilepton rates at the LHC and, for the time being, should be seen as part of our model. The assumption of having equal branchings of 1/3 in the decay of the scalar to all three lepton families allows to extend the universality of spin-1 bileptons also to the scalar sector, allowing to treat the two states (scalar and vector) on a similar footing. This option is clearly possible since we have 9 total parameters in the mass matrix which are constrained by 6 conditions. Three of them are necessary in order to reproduce the lepton masses and the remaining three come from the requirement of having equal values of the branching ratios of the scalars into the three lepton families. The explicit expressions of the solutions of such conditions are very involved and we have hence opted for a numerical scanning of the mass matrices satisfying such requirements. This in general requires that the ratio of the matrix elements of G_η over those of G_σ to be proportional to $v_\sigma/v_\eta \sim 10^{-2}$. Of course, if possible experimental data deviated significantly from $\text{BR}(l^\pm l^\pm) = 1/3$, then they would clearly favour a scalar bilepton, because lepton-flavour universality is mandatory for vector bileptons.

3.4. Physical Higgs bosons

The inclusion of the sextet representation in the potential enriches the phenomenology of the model and enlarges the number of physical states in the spectrum. In fact we now have, after electroweak symmetry breaking (EWSB) $SU(3)_L \times U(1)_X \rightarrow SU(2)_L \times U(1)_Y \rightarrow U(1)_{\text{em}}$, five scalar Higgses, three pseudoscalar Higgses, four charged Higgses and three doubly-charged Higgses. The (lepton-number conserving) potential of the model is given by [23]

$$\begin{aligned} V = & m_1 \rho^\dagger \rho + m_2 \eta^\dagger \eta + m_3 \chi^\dagger \chi + \lambda_1 (\rho^\dagger \rho)^2 + \lambda_2 (\eta^\dagger \eta)^2 + \lambda_3 (\chi^\dagger \chi)^2 + \lambda_{12} \rho^\dagger \rho \eta^\dagger \eta \\ & + \lambda_{13} \rho^\dagger \rho \chi^\dagger \chi + \lambda_{23} \eta^\dagger \eta \chi^\dagger \chi + \zeta_{12} \rho^\dagger \eta \eta^\dagger \rho + \zeta_{13} \rho^\dagger \chi \chi^\dagger \rho + \zeta_{23} \eta^\dagger \chi \chi^\dagger \eta \\ & + m_4 \text{Tr}(\sigma^\dagger \sigma) + \lambda_4 (\text{Tr}(\sigma^\dagger \sigma))^2 + \lambda_{14} \rho^\dagger \rho \text{Tr}(\sigma^\dagger \sigma) + \lambda_{24} \eta^\dagger \eta \text{Tr}(\sigma^\dagger \sigma) + \lambda_{34} \chi^\dagger \chi \text{Tr}(\sigma^\dagger \sigma) \\ & + \lambda_{44} \text{Tr}(\sigma^\dagger \sigma \sigma^\dagger \sigma) + \zeta_{14} \rho^\dagger \sigma \sigma^\dagger \rho + \zeta_{24} \eta^\dagger \sigma \sigma^\dagger \eta + \zeta_{34} \chi^\dagger \sigma \sigma^\dagger \chi \\ & + (\sqrt{2} f_{\rho\eta\chi} \epsilon^{ijk} \rho_i \eta_j \chi_k + \sqrt{2} f_{\rho\sigma\chi} \rho^T \sigma^\dagger \chi \\ & + \xi_{14} \epsilon^{ijk} \rho^{*l} \sigma_{li} \rho_j \eta_k + \xi_{24} \epsilon^{ijk} \epsilon^{lmn} \eta_i \eta_l \sigma_{jm} \sigma_{kn} + \xi_{34} \epsilon^{ijk} \chi^{*l} \sigma_{li} \chi_j \eta_k) + \text{h.c.} \end{aligned} \quad (36)$$

The EWSB mechanism will cause a mixing among the Higgs fields; from Eq. (36) it is possible to obtain the explicit expressions of the mass matrices of the scalar, pseudoscalar, charged and

doubly-charged Higgses, by using standard procedures. In the broken Higgs phase, the minimization conditions

$$\frac{\partial V}{\partial v_\phi} = 0, \quad \langle \phi^0 \rangle = v_\phi, \quad \phi = \rho, \eta, \chi, \sigma \quad (37)$$

will define the tree-level vacuum. We remind that we are considering massless neutrinos choosing the neutral field σ_1^0 to be inert. The explicit expressions of the minimization conditions are then given by

$$m_1 v_\rho + \lambda_1 v_\rho^3 + \frac{1}{2} \lambda_{12} v_\rho v_\eta^2 - f_{\rho\eta\chi} v_\eta v_\chi + \frac{1}{2} \lambda_{13} v_\rho v_\chi^2 - \frac{1}{\sqrt{2}} \xi_{14} v_\rho v_\eta v_\sigma + f_{\rho\sigma\chi} v_\chi v_\sigma \quad (38)$$

$$+ \frac{1}{2} \lambda_{14} v_\rho v_\sigma^2 + \frac{1}{4} \zeta_{14} v_\rho v_\sigma^2 = 0$$

$$m_2 v_\eta + \frac{1}{2} \lambda_{12} v_\rho^2 v_\eta + \lambda_2 v_\eta^3 - f_{\rho\eta\chi} v_\rho v_\chi + \frac{1}{2} \lambda_{23} v_\eta v_\chi^2 - \frac{1}{2\sqrt{2}} \xi_{14} v_\rho^2 v_\sigma + \frac{1}{2\sqrt{2}} v_\chi^2 v_\sigma \quad (39)$$

$$+ \frac{1}{2} \lambda_{24} v_\eta v_\sigma^2 - \xi_{24} v_\eta v_\sigma^2 = 0$$

$$m_3 v_\chi + \lambda_3 v_\chi^3 + \frac{1}{2} \lambda_{13} v_\rho^2 v_\chi - f_{\rho\eta\chi} v_\rho v_\eta + \frac{1}{2} \lambda_{23} v_\eta^2 v_\chi + \frac{1}{\sqrt{2}} \xi_{34} v_\eta v_\chi v_\sigma + f_{\rho\sigma\chi} v_\rho v_\sigma \quad (40)$$

$$+ \frac{1}{2} \lambda_{34} v_\chi v_\sigma^2 + \frac{1}{4} \zeta_{34} v_\chi v_\sigma^2 = 0$$

$$m_4 v_\sigma + \frac{1}{2} \lambda_{14} v_\rho^2 v_\sigma + \lambda_{44} v_\sigma^3 + \frac{1}{2} \lambda_4 v_\sigma^3 + f_{\rho\sigma\chi} v_\rho v_\chi - \frac{1}{2\sqrt{2}} \xi_{14} v_\rho^2 v_\eta + \frac{1}{2\sqrt{2}} \xi_{34} v_\eta v_\chi^2 \quad (41)$$

$$+ \frac{1}{2} \lambda_{14} v_\rho^2 v_\sigma + \frac{1}{4} \zeta_{14} v_\rho^2 v_\sigma + \frac{1}{2} \lambda_{24} v_\eta^2 v_\sigma - \xi_{24} v_\eta v_\sigma^2 + \frac{1}{2} \lambda_{34} v_\chi^2 v_\sigma + \frac{1}{4} \zeta_{34} v_\chi^2 v_\sigma = 0$$

These conditions are inserted into the the tree-level mass matrices of the CP-even and CP-odd Higgs sectors, derived from $M_{ij} = \partial^2 V / \partial \phi_i \partial \phi_j|_{v_{ev}}$, where V is the potential in Eq. (36): the explicit expressions of the mass matrices are too cumbersome to be presented here, although their calculation is rather straightforward. After a numerical diagonalization, we derive both the mass eigenstates and the Goldstone bosons.

In this case we have 5 scalar Higgs bosons, one of them will be the SM Higgs with mass about 125 GeV, along with 4 neutral pseudoscalar Higgs bosons, out of which 2 are the Goldstones of the Z and the Z' massive vector bosons. In addition there are 6 charged Higgses, 2 of which are the charged Goldstones and 3 are doubly-charged Higgses, one of which is a Goldstone boson. The Goldstones are exactly 8, as the massive vector bosons below the electroweak scale.

Hereafter we shall give the schematic expression of the physical Higgs states, after EWSB, in terms of the gauge eigenstates, whose expressions contain only the vev of the various fields. In the following equations, $R_{ij}^K \equiv R_{ij}^K(m_1, m_2, m_3, \lambda_1, \lambda_2, \dots)$ refers to the rotation matrix of each Higgs sector that depends on all the parameters of the potential in Eq. (36). Starting from the scalar (CP-even) Higgs bosons we have

$$H_i = R_{i1}^S \text{Re } \rho^0 + R_{i2}^S \text{Re } \eta^0 + R_{i3}^S \text{Re } \chi^0 + R_{i4}^S \text{Re } \sigma^0 + R_{i5}^S \text{Re } \sigma_1^0, \quad (42)$$

expressed in terms of the rotation matrix of the scalar components R^S . There are similar expressions for the pseudoscalars

$$A_i = R_{i1}^P \text{Im } \rho^0 + R_{i2}^P \text{Im } \eta^0 + R_{i3}^P \text{Im } \chi^0 + R_{i4}^P \text{Im } \sigma^0 + R_{i5}^P \text{Im } \sigma_1^0. \quad (43)$$

in terms of the rotation matrix of the pseudoscalar components R^P . Here, however, we have two Goldstone bosons responsible for the generation of the masses of the neutral gauge bosons Z and Z' given by

$$A_0^1 = \frac{1}{N_1} (v_\rho \text{Im } \rho^0 - v_\eta \text{Im } \eta^0 + v_\sigma \text{Im } \sigma^0), \quad N_1 = \sqrt{v_\rho^2 + v_\eta^2 + v_\sigma^2}; \quad (44)$$

$$A_0^2 = \frac{1}{N_2} (-v_\rho \text{Im } \rho^0 + v_\chi \text{Im } \chi^0), \quad N_2 = \sqrt{v_\rho^2 + v_\chi^2}. \quad (45)$$

For the charged Higgs bosons the interaction eigenstates are

$$H_i^\pm = R_{i1}^C \rho^\pm + R_{i2}^C (\eta^\mp)^* + R_{i3}^C \eta^\pm + R_{i4}^C (\chi^\mp)^* + R_{i5}^C \sigma_1^\pm + R_{i6}^C (\sigma_2^\mp)^* \quad (46)$$

with R^C being a rotation matrix of the charged sector. Even in this case we have two Goldstones because in the 331 model there are the W^\pm and the Y^\pm gauge bosons. The explicit expressions of the Goldstones are

$$H_W^\pm = \frac{1}{N_W} (-v_\eta \eta^\pm + v_\chi (\chi^\mp)^* + v_\sigma (\sigma_2^\mp)^*), \quad N_W = \sqrt{v_\eta^2 + v_\chi^2 + v_\sigma^2}; \quad (47)$$

$$H_Y^\pm = \frac{1}{N_Y} (v_\rho \rho^\pm - v_\eta (\eta^\mp)^* + v_\sigma \sigma_1^\pm), \quad N_Y = \sqrt{v_\rho^2 + v_\eta^2 + v_\sigma^2}. \quad (48)$$

In particular, we are interested in the doubly-charged Higgses, where the number of physical states, after EWSB, is three, whereas we would have had only one physical doubly-charged Higgs if we had not included the sextet. The physical doubly-charged Higgs states are expressed in terms of the gauge eigenstates and the elements of the rotation matrix R^C as

$$H_i^{++} = R_{i1}^{2C} \rho^{++} + R_{i2}^{2C} (\chi^{--})^* + R_{i3}^{2C} \sigma_1^{++} + R_{i4}^{2C} (\sigma_2^{--})^*. \quad (49)$$

In particular, the structure of the corresponding Goldstone boson is

$$H_0^{++} = \frac{1}{N} (-v_\rho \rho^{++} + v_\chi (\chi^{--})^* - \sqrt{2} v_\sigma \sigma_1^{++} + \sqrt{2} v_\sigma (\sigma_2^{--})^*) \quad (50)$$

where $N = \sqrt{v_\rho^2 + v_\chi^2 + 4v_\sigma^2}$ is a normalization factor.

3.5. Vertices for $H^{\pm\pm}$ and $Y^{\pm\pm}$

In Fig. 1 we present the typical contributions to the partonic cross section of the process $pp \rightarrow B^{++} B^{--}$, where $B^{\pm\pm}$ denotes either a spin-0 or a spin-1 bilepton; each $B^{\pm\pm}$ decays into a same-sign lepton pair. From Fig. 1, we learn that bilepton pairs can be produced in Drell–Yan processes mediated by either a vector boson ($V^0 = \gamma, Z, Z'$) or a scalar neutral Higgs ($h_1 \cdots h_5$); moreover, their production can be mediated by the exchange of an exotic quark Q in the t -channel as well. In principle, we may even have BB production via an effective vertex in gluon-gluon fusion, but this contribution turned out to be negligible with respect to the subprocesses with initial-state quarks.

In the following, we wish to discuss the differences between the couplings of scalar Higgses and vector bosons to scalar and vector bileptons, as the production rates at the LHC crucially depend on such couplings. Considering first the case of vector $Y^{\pm\pm}$, the Lorentz structure of the $V^0(p^1)Y^{++}(p^2)Y^{--}(p^3)$ vertex is given in terms of the momenta by

$$V(p_\mu^1, p_\nu^2, p_\rho^3) = g_{\mu\nu}(p_\rho^2 - p_\rho^1) + g_{\nu\rho}(p_\mu^3 - p_\mu^2) + g_{\mu\rho}(p_\nu^1 - p_\nu^3). \quad (51)$$

Characterizing the vector boson V as photon, Z or Z' , we obtain:

$$\begin{aligned}\gamma_\alpha Y_\mu^{++} Y_\nu^{--} &= -2ig_2 \sin \theta_W V(p_\alpha^\gamma, p_\mu^{Y^{++}}, p_\nu^{Y^{--}}) \\ Z_\alpha Y_\mu^{++} Y_\nu^{--} &= \frac{i}{2} g_2 (1 - 2 \cos 2\theta_W) \sin \theta_W V(p_\alpha^Z, p_\mu^{Y^{++}}, p_\nu^{Y^{--}}) \\ Z'_\alpha Y_\mu^{++} Y_\nu^{--} &= -\frac{i}{2} g_2 \sqrt{12 - 9 \sec^2 \theta_W} V(p_\alpha^{Z'}, p_\mu^{Y^{++}}, p_\nu^{Y^{--}}),\end{aligned}\tag{52}$$

where θ_W is the Weinberg angle.

In the case of the doubly-charged Higgs boson, the situation is slightly different: in fact, the interaction $V^0 H^{++} H^{--}$ is generated after that the Higgses take a vev. The Lorentz structure of the coupling will be of course proportional to the difference of the momenta of the Higgs fields. Defining $S(p_\mu^1, p_\mu^2) = p_\mu^1 - p_\mu^2$, we have

$$\begin{aligned}\gamma_\alpha H_i^{++} H_j^{--} &= -i \sin \theta_W \left[\left(g_2 + g_1 \sqrt{\cot^2 \theta_W - 3} \right) (R_{i1}^{2C} R_{j1}^{2C} + R_{i2}^{2C} R_{j2}^{2C}) \right. \\ &\quad \left. + 2g_2 (R_{i3}^{2C} R_{j3}^{2C} + R_{i4}^{2C} R_{j4}^{2C}) \right] S \left(p_\alpha^{H_i^{++}}, p_\alpha^{H_j^{--}} \right) \\ &= -2ie\delta_{ij} S \left(p_\alpha^{H_i^{++}}, p_\alpha^{H_j^{--}} \right)\end{aligned}\tag{53}$$

$$\begin{aligned}Z_\alpha H_i^{++} H_j^{--} &= \frac{i}{2} \sec \theta_W \left\{ \cos 2\theta_W \left(g_2 + g_1 \sqrt{\cot^2 \theta_W - 3} \right) - g_1 \sqrt{\cot^2 \theta_W - 3} \right\} R_{i1}^{2C} R_{j1}^{2C} \\ &\quad - 2 \left[\left(g_2 + g_1 \sqrt{\cot^2 \theta_W - 3} \right) \sin^2 \theta_W R_{i2}^{2C} R_{j2}^{2C} - g_2 \cos 2\theta_W R_{i3}^{2C} R_{j3}^{2C} \right. \\ &\quad \left. + 2g_2 \sin^2 \theta_W R_{i4}^{2C} R_{j4}^{2C} \right] S \left(p_\alpha^{H_i^{++}}, p_\alpha^{H_j^{--}} \right)\end{aligned}\tag{54}$$

$$\begin{aligned}Z'_\alpha H_i^{++} H_j^{--} &= \frac{i}{2} \frac{\sec^2 \theta_W}{\sqrt{12 - 9 \sec^2 \theta_W}} \left\{ \left[3g_1 \sqrt{\cot^2 \theta_W - 3} (\cos 2\theta_W - 1) + g_2 (2 \cos 2\theta_W - 1) \right] R_{i1}^{2C} R_{j1}^{2C} \right. \\ &\quad + \left[3g_1 \sqrt{\cot^2 \theta_W - 3} (\cos 2\theta_W - 1) + 2g_2 (2 \cos 2\theta_W - 1) \right] R_{i2}^{2C} R_{j2}^{2C} \\ &\quad \left. + 2g_2 (2 \cos 2\theta_W - 1) (R_{i3}^{2C} R_{j3}^{2C} + 2R_{i4}^{2C} R_{j4}^{2C}) \right\} S \left(p_\alpha^{H_i^{++}}, p_\alpha^{H_j^{--}} \right).\end{aligned}\tag{55}$$

The interactions shown in Eq. (52) and Eq. (53) are clearly very different, both in their Lorentz structures and in their dependence on the parameters of the model; therefore, different decay rates $V^0, h_i \rightarrow B^{++} B^{--}$ are to be expected, according to whether B is a scalar or a vector. It can be noticed that the expressions of the coupling in $\gamma Y^{++} Y^{--}$, i.e. $2g_2 \sin \theta_W \equiv 2e$, is apparently very different from the $\gamma H^{++} H^{--}$ one, but one can show that, after simplifications, they turn out to be the same, as expected. The relevant vertices for vector bileptons are

$$\ell \ell Y^{++} = \begin{Bmatrix} -\frac{i}{\sqrt{2}} g_2 \gamma^\mu & P_L \\ \frac{i}{\sqrt{2}} g_2 \gamma^\mu & P_R \end{Bmatrix}\tag{56}$$

$$\bar{d} T Y^{--} = \begin{Bmatrix} -\frac{i}{\sqrt{2}} g_2 \gamma^\mu & P_L \\ 0 & P_R \end{Bmatrix}\tag{57}$$

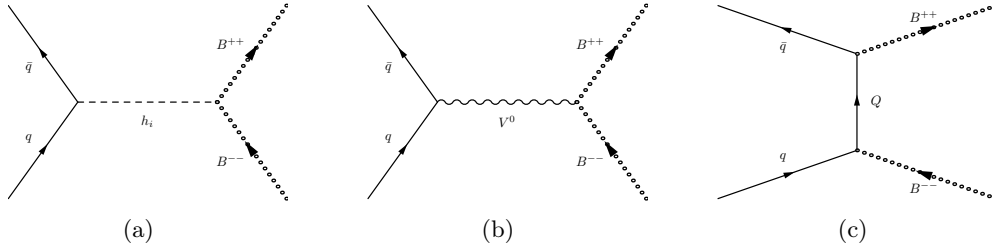


Figure 1: Typical contributions to events with two doubly-charged bosons in the final state and no extra jets. (a) and (b): contributions due to the mediation of a scalar (a) and a vector (b) boson. (c): t -channel exchange of exotic quarks Q .

$$\bar{D} u Y^{--} = \begin{Bmatrix} \frac{i}{\sqrt{2}} g_2 \gamma^\mu & P_L \\ 0 & P_R \end{Bmatrix} \quad (58)$$

$$h_i Y^{++} Y^{--} = \frac{i}{2} g_2^2 (v_\rho R_{i1}^S + v_\chi R_{i3}^S) \quad (59)$$

$$\gamma Y^{++} Y^{--} = -2i g_2 \sin \theta_W \quad (60)$$

$$Z Y^{++} Y^{--} = \frac{i}{2} g_2 (1 - 2 \cos 2\theta_W) \sec \theta_W \quad (61)$$

$$Z' Y^{++} Y^{--} = -\frac{i}{2} g_2 \sqrt{12 - 9 \sec^2 \theta_W}. \quad (62)$$

In the equations above, $P_{L,R}$ are the usual left- and right-handed projectors $P_{L,R} = (1 \mp \gamma_5)/2$.

4. Phenomenological analysis at the LHC

In this section we wish to present a phenomenological analysis, aiming at exploring possible scalar- or vector-bilepton signals at the LHC.

As in our previous work, we choose a specific benchmark point, obtained after scanning the parameter space by employing the **SARAH** 4.9.3 program and its **UFO** [28] interface. In doing so, we make use of the analytical expression of the mass matrices and of the minimization conditions of the potential in Eqs. (38)–(41). The mass eigenvalues are computed numerically, after varying all the quartic couplings in Eq. (36) between -1 and 1 and the vacuum expectation value v_ρ , responsible of the first breaking of the 331 model, between 2 and 4 TeV. Possible benchmark points are then chosen in such a way that all particle masses are positive, the SM-like Higgs boson has mass at about 125 GeV and one is consistent with the current LHC exclusion limits on new physics scenarios. Moreover, as discussed in [4], we require the couplings of the lightest neutral Higgs boson to the Standard Model fermions and bosons to be the same as in the Standard Model, within 10% accuracy. For the sake of comparison, we also choose the doubly-charged vectors and scalars to have roughly the same mass and just above the present ATLAS and CMS exclusion limits [17, 18] on doubly-charged Higgs bosons.. Furthermore, we are obviously interested in enhancing possible

Benchmark Point		
$m_{h_1} = 126.3 \text{ GeV}$	$m_{h_2} = 1804.4 \text{ GeV}$	$m_{h_3} = 2474.0 \text{ GeV}$
$m_{h_4} = 6499.8 \text{ GeV}$	$m_{h_5} = 6528.1 \text{ GeV}$	
$m_{a_1} = 1804.5 \text{ GeV}$	$m_{a_2} = 6496.0 \text{ GeV}$	$m_{a_3} = 6528.1 \text{ GeV}$
$m_{h_1^\pm} = 1804.5 \text{ GeV}$	$m_{h_2^\pm} = 1873.4 \text{ GeV}$	$m_{h_3^\pm} = 6498.1 \text{ GeV}$
$m_{h_1^{\pm\pm}} = 878.3 \text{ GeV}$	$m_{h_2^{\pm\pm}} = 6464.3 \text{ GeV}$	$m_{h_3^{\pm\pm}} = 6527.7 \text{ GeV}$
$m_{Y^{\pm\pm}} = 878.3 \text{ GeV}$	$m_{Y^\pm} = 881.8 \text{ GeV}$	$m_{Z'} = 3247.6 \text{ GeV}$
$m_D = 1650.0 \text{ GeV}$	$m_S = 1660.0 \text{ GeV}$	$m_T = 1700.0 \text{ GeV}$

Table 1: Benchmark point for our collider study, consistent with the $\sim 125 \text{ GeV}$ Higgs mass and the present exclusion limits on BSM physics.

331-model signals. Limiting ourselves to the Higgs and exotic sectors, the particle masses in our reference point are quoted in Table 1.

From Table 1, we learn that the 331 model, as expected, after including the sextet sector, yields 5 neutral scalar (h_1, \dots, h_5); 3 pseudoscalar (a_1, a_2 and a_3) and 3 singly-charged ($h_1^\pm, h_2^\pm, h_3^\pm$) Higgs bosons: the lightest h_1 is SM-like, whereas the others have mass between 1.8 and 6.5 TeV. In particular, h_2 is roughly degenerate with a_1 and h_1^\pm , while $h_4, h_5, a_2, a_3, h_2^\pm$ and h_3^\pm have all mass about 6.5 TeV. As for doubly-charged particles, both $Y^{\pm\pm}$ and $h_1^{\pm\pm}$ have mass around 878 GeV, just above the current exclusion limit for doubly-charged scalars, while the other scalars $h_2^{\pm\pm}$ and $h_3^{\pm\pm}$ are in the 6.5 TeV range and the singly-charged vector Y^\pm is roughly as heavy as the doubly-charged one. In our scenario, doubly-charged vectors and scalars decay only into lepton pairs, with branching ratio 1/3 for each lepton family ($ee, \mu\mu$ or $\tau\tau$). The exotic quarks D, S and T in our reference point have instead mass between 1.65 and 1.70 TeV. In principle, such exotic quarks can be produced in pairs at the LHC, with cross sections in the range of 0.5-0.7 fb at 13 TeV and 0.8-1.1 fb at 14 TeV, and may deserve a complete phenomenological analysis, especially in the high-luminosity LHC phase. Nevertheless, in the present paper we prefer to concentrate ourselves on the bilepton phenomenology and defer a thorough investigation on the production and decays of exotic quarks of charge 4/3 and 5/3 to future work [29].

The Z' boson deserves further comments. In [5] the relation

$$\frac{m_{Y^{++}}}{m_{Z'}} \simeq \frac{\sqrt{3 - 12 \sin^2 \theta_W}}{2 \cos \theta_W} \simeq 0.27 \quad (63)$$

was determined between Z' and vector-bilepton masses, and in fact in Table 1 Eq. (63) is verified to a pretty good accuracy. Moreover, in our benchmark scenario the Z' width is almost 700 GeV and, as found out in [30] when exploring Z' bosons in 331 models, our Z' is leptophobic. Therefore, the searches for Z' bosons carried out so far by ATLAS [26] and CMS [27], which have set exclusion limits around 4 TeV on their mass, cannot be directly applied to our scenario, since such searches were mostly performed for narrow resonances decaying into dilepton final states². In our reference

²See, e.g., Ref. [31] on how the Z' exclusion limits are modified in leptophobic models.

point, the Z' decays dominantly into $q\bar{q}$ pairs, amounting to almost 70% of the total width, and has a significant branching ratio into $Y^{++}Y^{--}$ pairs, about 14%; its decay rate into doubly-charged scalars $h_1^{++}h_1^{--}$ is instead rather small, roughly 1%. Such a difference can be easily explained in terms of the particle spins: the Z' has spin 1 and therefore, in the decay into $h_1^{++}h_1^{--}$, only the amplitude where the Z' has zero helicity with respect to the $h_1^{++}h_1^{--}$ axis contributes. On the contrary, in a possible decay into vector states $Z' \rightarrow Y^{++}Y^{--}$, amplitudes with helicity 0 and ± 1 with respect to the $Y^{++}Y^{--}$ direction play a role.

In the following, we shall present results for the production of two same-sign lepton pairs at the LHC, mediated by either vector or scalar bileptons in the 331 model:

$$pp \rightarrow Y^{++}Y^{--}(H^{++}H^{--}) \rightarrow (l^+l^+)(l^-l^-), \quad (64)$$

where $l = e, \mu$ and, for simplicity, we have denoted by $H^{\pm\pm}$ the lightest doubly-charged Higgs boson $h_1^{\pm\pm}$. The amplitude of process (64) is generated by the **MadGraph** code [15], matched with **HERWIG** 6 for shower and hadronization [16]. We have set $\sqrt{s} = 13$ TeV and chosen the NNPDFLO1 parton distributions [32], which are the default sets in **MadGraph**.

As in Ref. [4], and along the lines of [17, 18], we set the following acceptance cuts on the lepton transverse momentum (p_T), rapidity (η) and invariant opening angle (ΔR):

$$p_{T,l} > 20 \text{ GeV}, \quad |\eta_l| < 2.5, \quad \Delta R_{ll} > 0.1. \quad (65)$$

We point out that, since our signal originates from the decay of particles with mass almost 1 TeV, the final-state electrons and muons will be pretty boosted, and therefore the actual values of the cuts in (65) are not really essential, especially the transverse-momentum cut.³ At 13 TeV LHC, after such cuts are applied, the LO cross sections, computed by **MadGraph**, read

$$\sigma(pp \rightarrow YY \rightarrow 4l) \simeq 4.3 \text{ fb} ; \quad \sigma(pp \rightarrow HH \rightarrow 4l) \simeq 0.3 \text{ fb}. \quad (66)$$

Once again, the difference in the cross sections can be explained in terms of the spin of the intermediate bileptons. In the centre-of mass frame, in fact, for scalar production, only the matrix element where the vector (γ , Z and Z') has helicity zero with respect to the $H^{++}H^{--}$ direction contributes; for decays into $Y^{++}Y^{--}$ final states also the ± 1 helicity amplitudes are to be taken into account. For processes mediated by scalars ($h_i \rightarrow H^{++}H^{--}/Y^{++}Y^{--}$), the vector final states has still more helicity options since Y^{++} and Y^{--} can rearrange their helicities in a few different ways to achieve angular-momentum conservation, i.e. a total vanishing helicity in the centre-of-mass frame. We therefore confirm the findings of Ref. [11], where a higher cross section for vector-bilepton production with respect to the scalars was obtained at 7 and 14 TeV.

As for the background, final states with four charged leptons may occur through intermediate Z -boson pairs:

$$pp \rightarrow ZZ \rightarrow (l^+l^-)(l^+l^-). \quad (67)$$

After setting the same cuts as in (65), the LO cross section of the process (67) is given by

$$\sigma(pp \rightarrow ZZ \rightarrow 4l) \simeq 6.1 \text{ fb}. \quad (68)$$

³Our cuts are in fact a conservative choice of the so-called overlap-removal algorithm implemented by ATLAS to discriminate lepton and jet tracks [33].

In principle, within the backgrounds, one should also consider SM Higgs-pair production (hh), with $h \rightarrow l^+l^-$. However, because of the tiny coupling of the Higgs boson to electrons and muons, such a background turns out to be negligible.

Assuming a luminosity of 300 fb^{-1} , the number of same-sign electron/muon pairs in processes mediated by YY , HH and ZZ are $N(YY) \simeq 1302$, $N(HH) \simeq 120$, $N(ZZ) \simeq 1836$. Defining the significance s to discriminate a signal S from a background B as

$$s = \frac{S}{\sqrt{B + \sigma_B^2}}, \quad (69)$$

σ_B being the systematic error on B , which we estimate as $\sigma_B \simeq 0.1B$, we find that the YY signal can be separate from the ZZ background with a significance $s \simeq 6.9$, while HH production is overwhelmed by both Standard Model background ($s = 0.6$) and possible vector-bilepton pairs ($s = 0.9$).

At 14 TeV, the cross sections read: $\sigma(YY) \simeq 6.0 \text{ fb}$, $\sigma(HH) \simeq 0.4 \text{ fb}$ and $\sigma(ZZ) \simeq 6.6 \text{ fb}$, leading to $N(YY) \simeq 17880$, $N(HH) \simeq 1260$ and $N(ZZ) \simeq 19740$ events with 3000 fb^{-1} of data. Therefore, in the high-luminosity phase of the LHC, one will be able to discriminate vector-like bileptons from the background with a significance of about 9 standard deviations, while one is still unable to distinguish doubly-charged Higgses from YY ($s = 0.70$) or ZZ ($s = 0.64$) pairs.

Besides total cross sections and significances, computed employing the foreseen number of events, it is instructive studying some final-state observables, in order to understand how one can possibly detect (mostly vector-like) bileptons at LHC. In Fig. 2 we present the transverse momentum of the hardest and next-to-hardest lepton ($p_{T,1}$ and $p_{T,2}$), the invariant opening angle between them (ΔR), the rapidity of the hardest lepton (η_1), the invariant mass (m_{ll}) and the polar angle (θ_{ll}) between same-sign leptons. In any figure, the results corresponding to YY (black solid histogram) HH (red dotted histogram) and ZZ production (blue dashed histogram) are displayed. Unlike Ref. [4], where all our spectra were normalized to 1, in Fig. 2 all distributions are normalized in such a way that the height of each bin, such as $N(p_T)$, yields the expected number of events for such values of p_T , η , ΔR , θ and m_{ll} for a luminosity of 300 fb^{-1} and $\sqrt{s} = 13 \text{ TeV}$.

As one could foresee from the very cross section and significance evaluations, the general feature of such spectra is that the 331 signal can be discriminated from the ZZ background, while it is not possible to detect doubly-charged Higgs pairs as the leptonic spectra are always significantly below those yielded by ZZ background and YY -pair production. As for the transverse momenta ($p_{T,1}$ and $p_{T,2}$), the ZZ distributions are rather sharp and peak at low p_T , while those yielded by the HH and YY bileptons are much broader and peak about 1 TeV ($p_{T,1}$) and at roughly 700 ($p_{T,2}$, YY) and 800 GeV ($p_{T,2}$, HH). Such a result should have been expected, since the Z decays into different-sign, while $Y^{\pm\pm}$ and $H^{\pm\pm}$ into same-sign electrons and muons. As anticipated, for every value of p_T , the HH spectrum is well below the YY one.

Regarding the rapidity ($\eta_{1,l}$) distribution of the leading lepton, the 331-model spectra are narrower than the background and yield a larger event fraction around $\eta_{1,l} \simeq 0$. Once again, since the ZZ background and the YY signal predict a number of events of a similar order of magnitude, while those due to scalar pairs are much lower, the rapidity spectrum can be useful to detect possible vector bileptons, but not to separate them from doubly-charged Higgses.

As for the polar angle between same-sign leptons θ_{ll} , the YY -inherited spectrum is peaked around $\theta_{ll} \simeq 1.2 \simeq 70^\circ$, while the background is much broader and maximum at about $\theta \simeq 0.7 \simeq 40^\circ$; the Higgs-like signal is instead negligible.

Concerning the same-sign lepton invariant mass m_{ll} , it is of course easy to discriminate the 331 signals, peaking at $m_{ll} \simeq 900$ GeV, from the Z -pair background, which is instead a broad distribution, significant up to about 350 GeV and maximum around 70 GeV. As to the bileptons, both invariant-mass spectra are pretty narrow, which reflect the fact that Y^{++} and H^{++} have widths roughly equal to 7 GeV and 400 MeV, respectively.

The distribution of the invariant opening angle ΔR between the hardest and next-to-hardest leptons is rather broad for the background, significant for $0 < \Delta R < 6$, while YY pairs yield a distribution in the range $1 < \Delta R < 5$, which, for $\Delta R \simeq 3$, even leads to more events than the background. The HH signal is possibly visible only for $2 < \Delta R < 4$, but even in this range it is negligible with respect to the SM background and the YY signal.

Our conclusion is therefore that, as already argued in [4], the LHC will be sensitive to the spin-1 bileptons of the 331 model already at 13 TeV and 300 fb^{-1} , and even more in the high-luminosity regime. If the LHC does not see any bilepton, it may mean either that bileptons do not exist or that they are scalars, since we have shown that the production of doubly-charged Higgs bosons in the 331 model is overwhelmed by the SM background, as well as by vector bileptons.

5. Discussion

We explored scalar ($H^{\pm\pm}$) and vector ($Y^{\pm\pm}$) bileptons in the framework of the 331 model, which has the appealing features of predicting anomaly cancellation and treating differently the third quark family with respect to the first two. We focused on the family embedding in the minimal 331 model and paid special attention to its scalar content, and especially to the sextet sector, whose presence enriches the particle spectrum and, in particular, leads to the prediction of doubly-charged scalar Higgs bosons. Such scalar bileptons can possibly compete with vector bileptons as a source of same-sign lepton pairs at the LHC. In fact, previous investigations on vector bileptons, such as [8], had put exclusion limits on the mass of $Y^{\pm\pm}$ exploiting the experimental searches for scalar $H^{\pm\pm}$, as if the bilepton spin had a negligible effect on the expected and observed limits at 95% confidence level.

We implemented the 331 model, including the new sextet content, in a full Monte Carlo simulation framework and chose a benchmark point of the parameter space, consistently with the present exclusion limits on BSM physics. We studied jetless events, with doubly-charged vectors and scalars produced at the LHC in Drell–Yan interactions mediated by photons, Z , Z' and neutral Higgs bosons, as well as in processes where exotic quarks are exchanged in the t -channel.

It was found that vector bileptons can be produced with a significant cross section already in the present LHC run at 13 TeV and that they can be easily discriminated from the SM background, by exploring distributions like the lepton transverse momentum, invariant mass, rapidity or invariant opening angle. The production of doubly-charged scalars is in principle interesting, but, because of the helicity suppression, its cross section is too low for them to be substantially visible at the LHC and separable from the background and the vector-bilepton signal.

Our study therefore confirms that, as already anticipated in a previous analysis, the production of vector-bilepton pairs is the striking feature of the 331 model and we believe that, given the large cross section and easy separation from the background, with a significance between 6σ and 9σ , it should deserve a full experimental search. As for doubly-charged scalars, although the 331 framework discussed in this work leads to a too low production cross section at the LHC, in order to achieve angular-momentum conservation, we plan to explore how much this conclusion depends on the actual setup for the family embedding and on the choice of the reference point, and whether

there could be other realizations of the model yielding a visible LHC rate even for scalar bileptons. Besides, it will be very interesting to study the phenomenology of the exotic quarks predicted by our 331 model and the LHC significance reach, especially in the high-luminosity and high-energy phases. This is in progress as well.

Acknowledgement

We acknowledge Antonio Sidoti for discussions on the cuts implemented in Eq. (65) and on the overlap-removal algorithm implemented by the ATLAS Collaboration. This work is partially supported by INFN ‘Iniziativa Specifiche’ QFT-HEP and ENP.

References

- [1] P.H. Frampton, *Chiral Dilepton Model and the Flavor Question*. Phys. Rev. Lett. **69**, 2889 (1992).
- [2] F. Pisano and V. Pleitez, *An $SU(3) \times U(1)$ Model of Electroweak Interactions*, Phys. Rev. **D46**, 410 (1992).
- [3] M. Singer, J.W.F. Valle and J. Schechter, *Canonical Neutral Current Predictions from the Weak Electromagnetic Group $SU(3) \times U(1)$* , Phys. Rev. **D22**, 738 (1980).
- [4] G. Corcella, C. Corianò, A. Costantini and P. H. Frampton, *Bilepton Signatures at the LHC*. Phys. Lett. B **773** (2017) 544. [arXiv:1707.01381 \[hep-ph\]](#).
- [5] B. Dion, T. Grégoire, D. London, L. Marleau, and H. Nadeau, *Bilepton Production at Hadron Colliders*, Phys. Rev. **D 59**, 075006 (1999). [arXiv:hep-ph/9810534](#).
- [6] E. Ramirez Barreto, Y. A. Coutinho and J. Sá Borges, *Vector-Bilepton Contribution to Four Lepton Production at the LHC*, Phys. Rev. **D88**, 035016 (2013), [arXiv:1307.4683\[hep-ph\]](#).
- [7] A. Alves, E. Ramirez Barreto and A.G. Dias, *Jets Plus Same-Sign Dileptons Signatures from Fermionic Leptoquarks*, Phys. Rev. **D86**, 055025 (2012), [arXiv:1203.3242\[hep-ph\]](#).
- [8] A.A. Nepomuceno, F.L. Eccard and B. Meirose, *First results on bilepton production based on LHC collision data and predictions for run II*, Phys. Rev. **D94** (2016) 055020.
- [9] ATLAS Collaboration, *Search for doubly-charged Higgs bosons in like-sign dilepton final states at $\sqrt{s} = 7$ TeV with the ATLAS detector*, Eur. Phys. J. **C72** (2012) 2244.
- [10] A. Alloul, M. Frank, B. Fuks, M. Rausch de Traubenberg, *Doubly-charged particles at the Large Hadron Collider*, Phys. Rev. **D88** (2013) 075004.
- [11] E. Ramirez Barreto, Y.A. Coutinho and J. Sá Borges, *Vector- and scalar-bilepton pair production in hadron colliders*, Phys. Rev. **D83** (2011) 075001.
- [12] M.D. Tonasse, *Decay properties of a class of doubly charged Higgs bosons*, Phys. Lett. **B718** (2012) 86.
- [13] J.A.M. Vermaseren, *New features of FORM*, math-ph/0010025.
- [14] F. Staub, *SARAH 4 : A tool for (not only SUSY) model builders*. Comput. Phys. Commun. **185** (2014) 1773 doi:10.1016/j.cpc.2014.02.018 [arXiv:1309.7223 \[hep-ph\]](#).
- [15] J. Alwall et al., *The automated computation of tree-level and next-to-leading order differential cross sections, with their matching to parton shower simulations*. JHEP **1407** (2014) 079 doi:10.1007/JHEP07(2014)079 [arXiv:1405.0301 \[hep-ph\]](#).
- [16] G. Corcella et al, *HERWIG 6: An Event generator for hadron emission reactions with interfering gluons (including supersymmetric processes)*, JHEP **0101** (2001) 010 doi:10.1088/1126-6708/2001/01/010 [hep-ph/0011363].
- [17] ATLAS Collaboration, *Search for doubly charged Higgs boson production in multi-lepton final states with the ATLAS detector using proton-proton collisions at $\sqrt{s} = 13$ TeV*, Eur. Phys. J. **C78** (2018) 199.
- [18] CMS Collaboration, *A search for doubly-charged Higgs boson production in three and four lepton final states at $\sqrt{s} = 13$ TeV*, CMS-PAS-HIG-16-036.
- [19] J. C. Pati and A. Salam, *Lepton Number as the Fourth Color*, Phys. Rev. **D10** (1974) 275, Erratum: Phys. Rev. **D11** (1975) 70.
- [20] R. N. Mohapatra and J. C. Pati, *Left-Right Gauge Symmetry and an Isoconjugate Model of CP Violation*, Phys. Rev. **D11** (1975) 566.
- [21] M. Muhlleitner and M. Spira, *Note on doubly charged Higgs pair production at hadron colliders*, Phys. Rev. **D68** (2003) 117701.
- [22] Q. H. Cao, Y. Liu, K. P. Xie, B. Yan and D. M. Zhang, *Diphoton excess, low energy theorem, and the 331 model*. Phys. Rev. **D 93** (2016) 075030.

- [23] M. B. Tully and G. C. Joshi, *Int. J. Mod. Phys. A* **18** (2003) 1573 doi:10.1142/S0217751X03013995 [hep-ph/9810282].
- [24] A.G. Dias, R. Martinez and V. Pleitez, *Concerning the Landau pole in 3-3-1 models*, *Eur. Phys. J.* **C39** (2005) 101.
- [25] R. Martinez and F. Ochoa, *The Landau pole and Z' decays in the 331 dilepton model*, *Eur. Phys. J.* **C51** (2005) 101.
- [26] ATLAS Collaboration, *Search for new high-mass phenomena in the dilepton final state using 36 fb⁻¹ of proton-proton collision data at $\sqrt{s} = 13$ TeV with the ATLAS detector*, *JHEP* **1710** (2017) 182.
- [27] CMS Collaboration, *Search for high-mass resonances in dilepton final states in proton-proton collisions at $\sqrt{s} = 13$ TeV*, CMS-EXO-16-047, CERN-EP-2018-027.
- [28] C. Degrande, C. Duhr, B. Fuks, D. Grellscheid, O. Mattelaer and T. Reiter, *UFO - The Universal FeynRules Output*, *Comput. Phys. Commun.* **183** (2012) 1201.
- [29] G. Corcella, A. Costantini, M. Ghezzi, L. Panizzi and G.M. Pruna, in preparation.
- [30] D. Gomez Dumm, *Leptophobic Character of the Z-prime in an $SU(3)_C \times SU(3)_L \times U(1)_X$ Model*, *Phys. Lett. B* **411** (1997) 313.
- [31] J.Y. Araz, G. Corcella, M. Frank and B. Fuks, *Loopholes in Z' searches at the LHC: exploring supersymmetric and leptophobic scenarios*, *JHEP* **1802** (2018) 092.
- [32] R. D. Ball et al. [NNPDF Collaboration], *Parton distributions with QED corrections*, *Nucl. Phys. B* **877**, 290 (2013).
- [33] A. Sidoti, private communication.

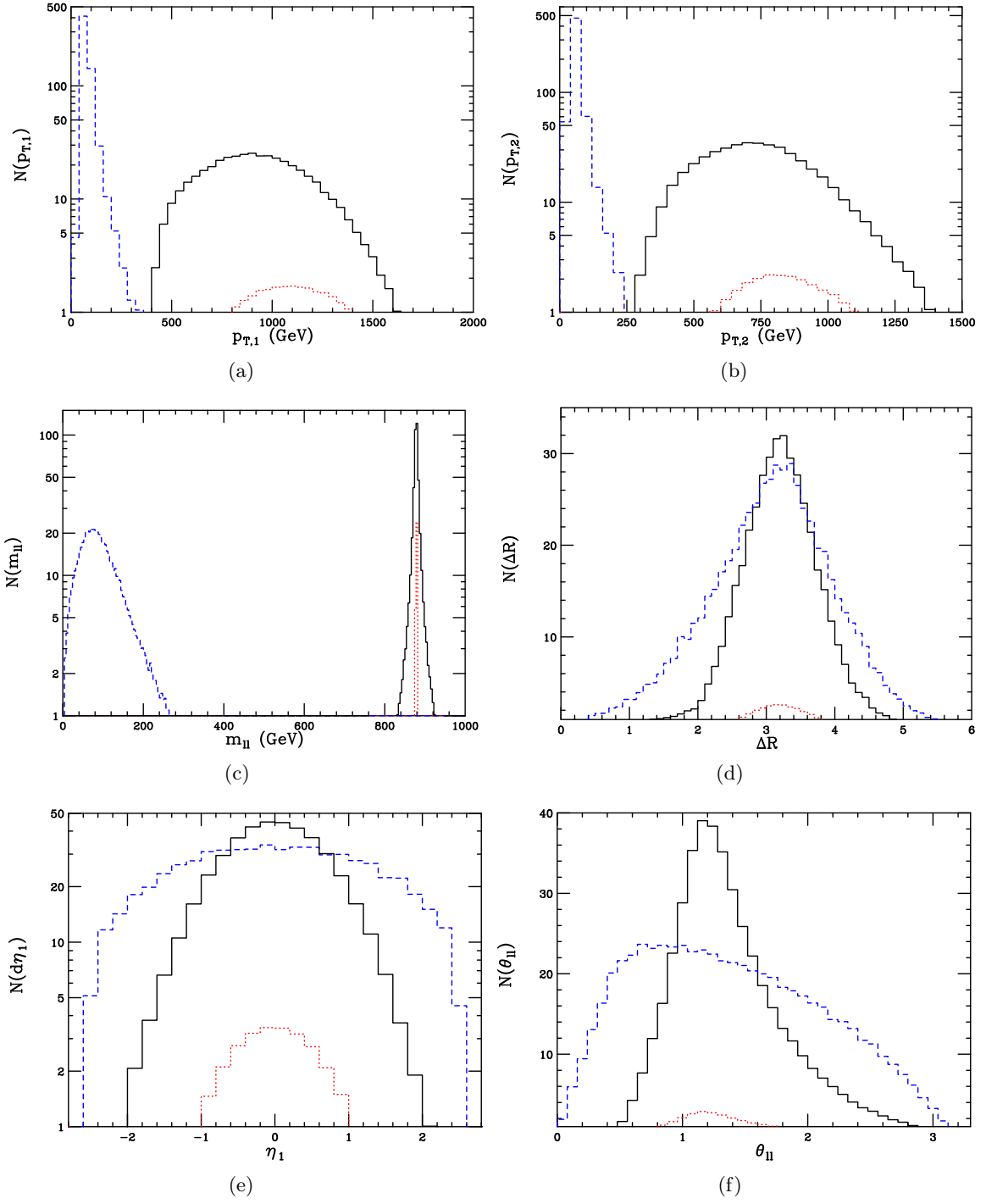


Figure 2: Distributions of the transverse momentum of the hardest (a) and next-to-hardest lepton (b), same-sign lepton invariant mass (c), invariant opening angle between the two hardest leptons (d), rapidity of the leading lepton (e), polar angle between same-sign leptons (f). The solid blue histograms are the spectra yielded by vector bileptons, the red dots correspond to scalar doubly-charged Higgs bosons, the blue dashes to the ZZ Standard Model background.